RADIATION RESEARCH **182**, 322–330 (2014)
0033-7587/14 $15.00

DOI: 10.1667/RR13664.1

Modeling Dose Deposition and DNA Damage Due to Low-Energy β^- Emitters

D. Alloni,[a,b,c,1] C. Cutaia,[a] L. Mariotti,[a,c] W. Friedland[d] and A. Ottolenghi[a,c]

[a] *Department of Physics, University of Pavia, 27100, Pavia, Italy;* [b] *LENA, Laboratory of Applied Nuclear Energy, University of Pavia, 27100, Pavia, Italy;* [c] *INFN National Institute of Nuclear Physics, Sezione di Pavia, 27100, Pavia, Italy; and* [d] *Institute of Radiation Protection, Helmholtz Zentrum München, Ingolstädter Landstrasse 1, 85764 Oberschleissheim, Neuherberg, Germany*

Alloni, D., Cutaia, C., Mariotti, L., Friedland, W. and Ottolenghi, A. Modeling Dose Deposition and DNA Damage due to Low-Energy β^- Emitters. *Radiat. Res*. 182, 322–330 (2014).

One of the main issues of low-energy internal emitters concerns the very short ranges of the beta particles, versus the dimensions of the biological targets. Depending on the chemical form, the radionuclide may be more concentrated either in the cytoplasm or in the nucleus of the target cell. Consequently, since in most cases conventional dosimetry neglects this issue it may overestimate or underestimate the dose to the nucleus and hence the biological effects. To assess the magnitude of these deviations and to provide a realistic evaluation of the localized energy deposition by low-energy internal emitters, the biophysical track-structure code PARTRAC was used to calculate nuclear doses, DNA damage yields and fragmentation patterns for different localizations of radionuclides in human interphase fibroblasts. The nuclides considered in the simulations were tritium and nickel-63, which emit electrons with average energies of 5.7 (range in water of 0.42 μm) and 17 keV (range of 5 μm), respectively, covering both very short and medium ranges of beta-decay products. The simulation results showed that the largest deviations from the conventional dosimetry occur for inhomogeneously distributed short-range emitters. For uniformly distributed radionuclides selectively in the cytoplasm but excluded from the cell nucleus, the dose in the nucleus is 15% of the average dose in the cell in the case of tritium but 64% for nickel-63. Also, the numbers of double-strand breaks (DSBs) and the distributions of DNA fragments depend on subcellular localization of the radionuclides. In the low- and medium-dose regions investigated here, DSB numbers are proportional to the nuclear dose, with about 50 DSB/Gy for both studied nuclides. In addition, DSB numbers on specific chromosomes depend on the radionuclide localization in the cell as well, with chromosomes located more peripherally in the cell nucleus being more damaged by short-ranged emitters in cytoplasm compared with chromosomes located more centrally. These results illustrate the potential for over- or underestimating the risk associated with low-energy emitters, particularly for tritium intake, when their distribution at subcellular levels is not appropriately considered.

[1] Address for correspondence: Laboratory of Applied Nuclear Energy, University of Pavia, Via Aselli 41, Pavia I-27100, Italy; e-mail: daniele.alloni@unipv.it.

INTRODUCTION

Internal radiation dosimetry has a fundamental role in the planning of nuclear medicine therapies and in diagnosis with radionuclides. For therapy, the rationale is to destroy pathologic tissues by irradiation with properly chosen radionuclides, while sparing other organs and tissues from unnecessary exposure (*1*). Proper pharmaceutical drugs are chosen for their ability to concentrate in target tissues and to therefore be labeled with a suitably chosen radionuclide. The best radionuclide is chosen based on its potential to maximize the radiation energy deposition in the target tissue during the desired treatment time. Beta emitters are the best choice in most cases, because beta radiation has a mean range in tissue from a few millimeters to a few centimeters.

The absorbed dose to target tissues, as well as to other organs, depends on the biokinetics of the radiopharmaceutical and the decay scheme of the adopted radionuclide (*2, 3*). While the physical properties of each nuclide are well known from experimental data, the biodistribution of the radiopharmaceutical within the patient's body depends on the dynamic biologic pathway that in turn is mainly governed by the role of the radiolabeled molecule (*4*). On a microscopic level, one of the main problems arises from the possible risks related to the physical inhomogeneities of the radiation source (*5*). These inhomogeneities might be due to the different diffusion of the beta emitters either because of the different diffusivity of the carrier [i.e., different organically bound tritium molecules (OBT)] or because of the physical barriers represented by the cellular and nuclear membranes. Radiation from these sources are capable of inducing detrimental biological effects (e.g., cancer) due to the damage caused by the ionization of cellular constituents, such as the DNA molecule and the chromosomes (*6*). Internal irradiation deposited by radionuclides is mostly due to short-range charged particle

TABLE 1
Main Characteristics of the Beta Emitters, Tritium (^{3}H) and Nickel-63 (^{63}Ni) used in the Simulations

Nuclide	Tritium	Nickel-63
Half life (physical)	12.33 years	100 years
Half life (biological)	≈10 days	≈500 days
E_{max}	18.6 keV	66 keV
E_{ave}	5.7 keV	17 keV
R_{max}	≈5.2 μm	≈20 μm
R_{ave}	≈0.42 μm	≈5 μm

Note. E_{max} and E_{ave}, and R_{max} and R_{ave} indicate the maximum and average energy of the associated beta particle, respectively.

emissions (e.g., low-energy beta or alpha emitters) and therefore its contribution to radiation dose and cellular damage, depends on the activity and concentration of the radionuclide and its location within tissues and cells (*7*).

In particular, incorporated low-energy β⁻-decaying radionuclides emit electrons with a range comparable to the size of the cell nucleus and of the genomic DNA, one of the most important biological targets. These radionuclides, depending on the chemical form, might be present at different locations in the nucleus or in the cytoplasm of a cell. If the radionuclide is concentrated in the cytoplasm, then conventional dosimetry, which assumes a uniform distribution of energy deposition starting events, will overestimate the dose to the nucleus, however, if the radionuclide is concentrated in the nucleus, there is a risk of underestimation of the dose to the nucleus (*7*).

Similar to low-energy beta emitters, Auger emitters also have unique properties related to dosimetric calculations. Briefly, these unique properties of Auger emitters are mostly due to the dense cascade of electrons released after radionuclide decay by electron capture and/or internal conversion. Most of these electrons are short-range particles with energies of less than 1 keV and the release of these electrons results in a deposition of large amounts of energy near the decay site resembling the characteristics of high-LET radiations (*8*). However, use of Auger emitting radionuclides presents major problems in dosimetry, in cancer therapy and diagnostic work. For example, in dosimetry, auger dose calculation is problematic since electronic equilibrium is not achieved at molecular size targets (*9*). Recent works (*10–13*) on track structure simulations of damage and repair for low-energy electrons have provided an overview on the modeling and calculation of DNA damage induced by Auger electrons and related cell dosimetry (*14*).

To further quantify these effects, we have performed here a systematic study through a series of simulations with a recently modified version of the Monte Carlo code PARTRAC (*15–17*) to calculate the dose and DNA damage in the nucleus for different concentrations of radionuclides in the nucleus and cytoplasm. The code implementation followed three main steps: 1. Testing of the source beta spectra; 2. Implementation of a new ''*ad hoc*'' source geometry for source distribution within the cell (nucleus, cytoplasm or both); and 3. Development of a new algorithm capable of quantifying the damage induced on different chromosomes by radiation exposure from different radionuclide distributions. In particular, we show that we can perform analysis on the results obtained from the simulations with the program that provide output files that are able to calculate the number of double-strand breaks (DSBs) per chromosome, and also allow us to verify that different distributions of radionuclides in the cell can induced damage to chromosomes that are quantitatively and qualitatively different. The radionuclides considered in this work were tritium (^{3}H) and nickel-63 (^{63}Ni), representing the ranges of very low- and medium-beta energies. As an isotope of hydrogen, tritium can be found as a constituent atom in the water molecule and basically in every organic compound (*18–21*). Tritium (^{3}H), which is radioactive, is found in nature and can also be produced by man-made processes (*22*). It decays to an isotope of helium (^{3}He) emitting a low-energy beta particle. The average range of the emitted beta particle in water (or equivalent biological tissues) is about 0.5 μm, considerably less than the typical diameter (5–20 μm) of a cell or even of a mammalian cell nucleus (*23–25*). The subcellular location of tritium atoms is therefore of utmost importance for understanding late biological effects. Moreover, because of its low initial energy and short range, the average density of ionizations produced by the passage of a tritium beta particle (mean LET = 12.1 keV/μm) is higher than the one for a moderate-/high-energy beta particle (*26–30*). For example, the mean LET for beta particles emitted from ^{90}Sr with 546 keV decay energy is 0.52 keV/μm. Therefore, although tritium is normally classified as a ''low-LET'' beta emitter, in reality its emission is intermediate between typical low-LET radiation (~ 0.5 keV/μm) and the high LET of an alpha particle. Tritium can be regarded as an extreme case of a radionuclide for which the chemical speciation is crucial in determining the biological effects of its radioactive decay. This is due to both the very wide spectrum of compounds in which the tritium atom may be firmly bound, and to the unusually short range of its emitted beta particles. The radioactive isotope nickel-63 is mainly artificially produced in nuclear reactors by neutron activation of nickel-62. Data found in Table 1 summarizes some of the characteristics of the tritium and nickel-63 radionuclides used to perform the simulation in this work (*26–28*).

MATERIALS AND METHODS

PARTRAC Biophysical Simulation Tool

In this study we used the biophysical Monte Carlo code PARTRAC (*8*), which enables simulation of electron and photon tracks with energies in the range of 10 eV–100 MeV, and also of proton and heavier ion tracks in the nonrelativistic regime. PARTRAC is based on an ''event-by-event'' description of radiation track structure in liquid water at the nanometer level, combined with an atom-by-atom

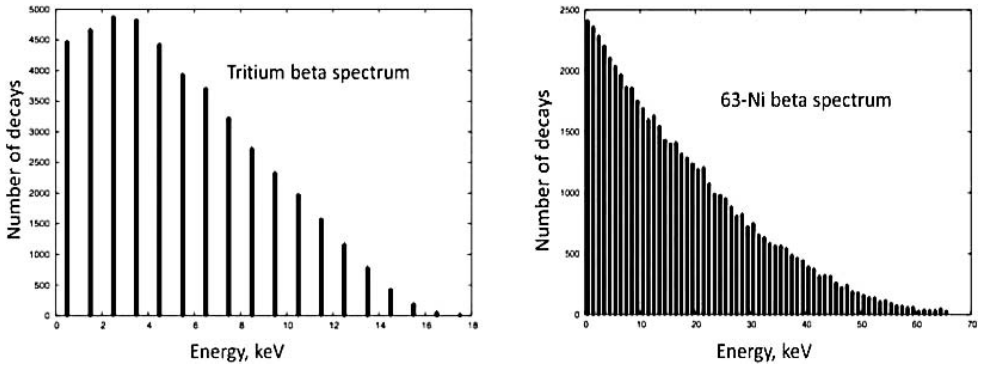

FIG. 1. Simulated beta spectra for tritium (left panel) and for nickel-63 (right panel) used as input in the PARTRAC code.

simulation of the biological target. The target is the whole genome of a human cell in its interphase and it is structured in six levels of DNA organization (deoxynucleotide pair, double helix, nucleosome, chromatin fiber, chromatin fiber loops and chromosome territories). The yields of radiation-induced DNA strand breaks were determined by superimposing the simulated track structure pattern on the DNA target model and it was assumed that if an inelastic energy deposition occurs in the volume occupied by the sugar-phosphate backbone or in the water shell surrounding the double helix, a single-strand break (SSB) may be produced if the energy released is larger than 5 eV (direct and quasi-direct effect, respectively). The probability of producing an SSB was assumed to increase linearly from 0–1 for energy depositions in the range of 5–40 eV and to be equal to 1 for energy depositions larger than 40 eV. For indirect effects, ionized water molecules were assumed to dissociate following the scheme $H_2O^+ + H_2O \rightarrow H_3O^+ + {}^{\bullet}OH$, whereas excited water molecules were assumed to undergo either relaxation or dissociation in the prechemical stage (*31*). During the chemical stage, diffusion and interactions (with each other) of reactive species were considered in a step-by-step approach (*32*). An interaction between an ${}^{\bullet}OH$ and a sugar phosphate was assumed to induce an SSB with 65% probability. Two SSBs on subsequent nucleotides in the same strand were considered as one SSB, whereas a DSB was assumed to occur when two SSBs occurred on sites directly opposite each other within 10 bp. Further details on the physics, chemistry and biology models embedded in PARTRAC can be found in a recent review (*17*).

PARTRAC Extension to Internal Emitters and their Inhomogeneous Intracellular Localization

To simulate the transport of electrons coming from beta emission of tritium or nickel-63 inside a cell, we first modified the part of the code that selects the energy of the emitted particles, introducing the energy spectra shown in Fig. 1, used as a discrete approximation to the continuous beta spectra. The second step was the extension of the code to locate the sources of beta particles within the cell volume and in different regions of the target volume (nucleus and/or cytoplasm).

PARTRAC Simulations

The geometrical setup of the reported study corresponds to a human cell with nucleus and cytoplasm volumes represented by concentric cylinders with base radius 7.5 μm wide and 5 μm high, and base radius 12.5 μm wide and 15 μm high, respectively. For the density of both cell and nucleus a value of 1.06 g/cm^3 was chosen. The volume outside the nuclear volume but inside the cell represented the cytoplasm, filled with liquid water as a surrogate for biological medium in the track simulations. Inside the nucleus, DNA and chromosomes are located according to the spherical chromatin domain (SCD) model (*33, 34*).

For each simulation, beta sources were randomly distributed, changing the concentration of the emitters (i.e., the numbers of starting points of the primary beta-particle tracks) between the cell nucleus and/or the cytoplasm. By varying the ratio $R = C_N/C_C$ of the emitter concentration in the nucleus (C_N) and in the cytoplasm (C_C), it was possible to simulate the behavior of specific radionuclides, either when they tend to be located predominantly in the nucleus as is the case when chemically bound to some organic molecule (e.g., OBT), or throughout the rest of the cell as has been described in studies with tritiated thymidine (*22*). R values also take into account the barrier effects due to the different (nuclear and cellular) membranes, which lead to different nuclide concentrations in the different cellular compartment, i.e., nucleus and cytoplasm. Beta-particle tracks were simulated until the total energy deposition in the cell amounted to a predefined ''cell dose'': 5.34 Gy, 2.14 Gy, 1.07 Gy and 0.53 Gy for tritium and 5.33 Gy, 2.12 Gy, 1.05 Gy and 0.56 Gy for nickel-63, respectively. The slight differences between the dose levels for the two nuclides arise from their different electron spectra. For simplicity, we have used the term ''dose,'' even for volumes as small as the cell or its nucleus, although the microdosimetry terminology of imparted specific energy is more precise and should actually be used here.

Each point in the graphs shown here was obtained from at least ten simulation runs and errors were calculated as standard deviations. To reduce the inter-simulation variations inherent in stochastic calculations, some simulations were performed with the cell dose of 100 Gy for nuclides located in the cytoplasm ($R = 0$; resulting in a ''nucleus dose'' of about 16 and 64 Gy for electrons emitted by the decay of tritium and nickel-63, respectively). For nuclides located homogeneously in the whole cell ($R = 1$), the cell doses for tritium and nickel-63 were 16 and 64 Gy, respectively; for homogeneously distributed emitters, the cell dose equals the ''nucleus dose,'' and therefore allows for direct comparison of the dose and DSB distribution for different values of R. Simulations for intermediate R values have combined the results of these two basic modes.

In addition to scoring energy deposition events in the nucleus and cytoplasm regions and thus quantifying the nucleus and cell doses, a number of biologically relevant end points have been considered in this work, which correspond to the induced DNA damage, namely: the total number of DSB, the yields of fragments in different size intervals and the DSB yields on individual chromosomes. Later additional end points that can be scored by PARTRAC, namely DSB repair and formation of chromosome aberrations, are beyond the scope of this current study.

For assessing DNA fragmentation, each DNA fragment (i.e., segment between two DSBs or a DSB and either a chromosome end or an intact chromosome) was tallied into different size ranges (see Results section), which correspond to the ones used in previous

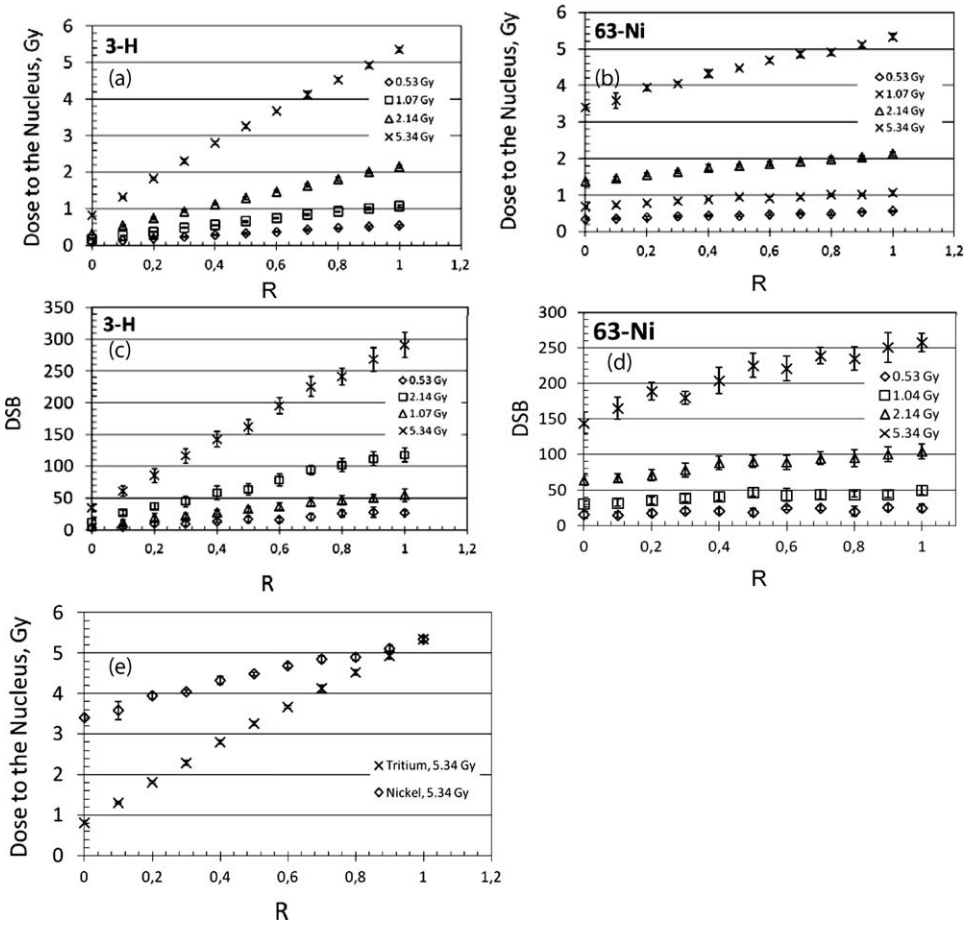

FIG. 2. As a function of the ratio R between the emitter concentrations in the nucleus and in the cytoplasm: Dose to the nucleus for tritium (panel a) and nickel-63 (panel b); number of DSBs for tritium (panel c) and nickel-63 (panel d). Different curves correspond to different total doses. Panel e: Comparison between the dose to the nucleus as a function of R for nickel-63 and tritium for the same dose of 5.34 Gy.

simulations and experimental works that led to the validation of PARTRAC (*16*). In particular, fragmentation analysis was performed using the output data set of the PARTRAC effect module containing the genomic positions of DSBs. The number of double-stranded fragments for each fragment size range was determined by calculating the distances between adjacent breaks or between a break and a chromosome end.

RESULTS

In this sections we present the results obtained from the simulations of ^{3}H and ^{63}Ni, together with considerations regarding the comparison between the effects due to the two different radionuclide energies.

Dose Deposition for Different 3H Concentrations in the Cell Nucleus

The dose deposited into the nucleus, which represents the most sensitive region in the cell for biological effects, as a function of the ratio R of the concentration of tritium in the nucleus (C_N) and in the cytoplasm (C_C) (Fig. 2a). Overall, the simulations exhibit an expected trend of linearity. Given that the range of the electrons with average energy of 5.7 keV is less than 0.5 μm, the nuclear dose arises mainly from the tracks starting (and located) within the nucleus, whose number is directly proportional to the nucleus-to-cytoplasmic concentration ratio R. The contribution to nuclear dose from electron tracks starting in the cytoplasm is not completely negligible, as shown by y axis intercepts in Fig. 2a, e.g., 0.82 Gy for the curve with cell dose of 5.34 Gy. The intercept, i.e., the nucleus dose value at $R = 0$, corresponds to tracks originating from emitters located in cytoplasm only. Nevertheless, parts of some of the tracks enter the nucleus and contribute to the energy deposited there. Even for the short-range electrons (mean range below 0.5 μm) generated by decays of tritium homogeneously distributed in the cytoplasm only, the nucleus dose amounts to about 15% of the cell-averaged dose (0.82 vs. 5.34 Gy). The nuclear dose corresponding to the case when tritium is homogeneously distributed in the whole cell ($R = 1$, uniform distribution of track starting points inside the cell) takes, as expected, the value of 5.34 Gy. This value equals the average dose to the cell, because in the homogeneous case the condition of electronic equilibrium in the nucleus is

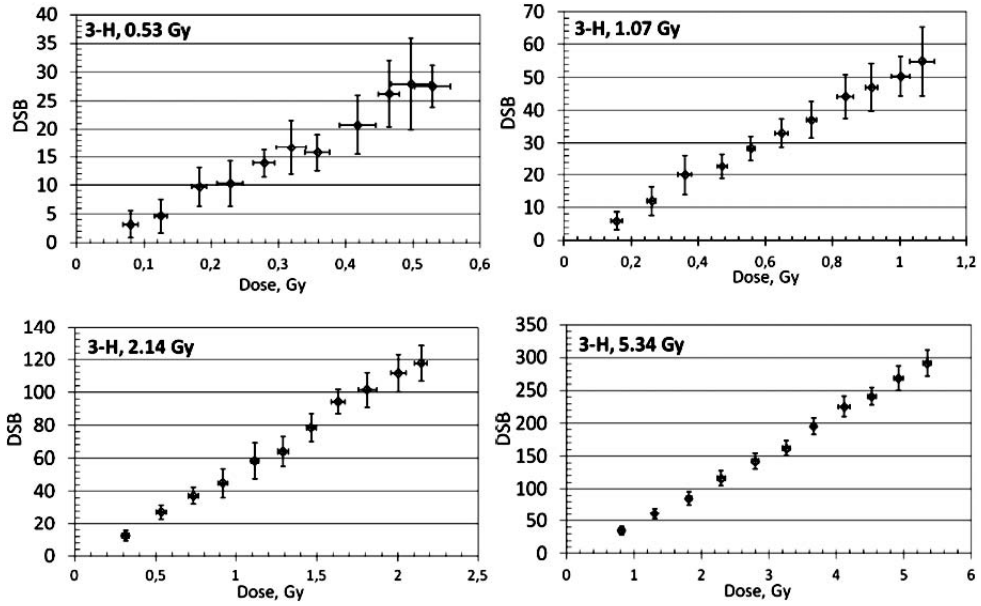

FIG. 3. Number of DSBs as a function of the dose to the nucleus for different uniform dose values for tritium.

satisfied, i.e., tracks that originate in the nucleus but escape outside are compensated by those starting in the cytoplasm and entering the nucleus. In contrast, in the case of homogeneously distributed emitter the cytoplasm dose is slightly smaller (5 Gy) than the cell dose, as some electron tracks protrude outside the cell and are not compensated for by tracks entering from outside, given the single-cell nature of the simulation. The same discussion also applies for lower doses (2.14, 1.07 and 0.53 Gy), and the intercepts are rescaled by the mean doses deposited to the cell and correspond to 0.31, 0.16 and 0.08 Gy, respectively.

DSB Induction and DNA Fragment Distributions for Different Intracellular Localizations of Tritium

As expected, for a fixed cell dose, the total number of DSBs increased with increasing nuclear-to-cytoplasmic location ratio R (Fig. 2c), mainly due to the increase in the number of tracks in the nucleus. In fact, in the dose range considered, the contribution of inter-track effects to DSB induction is negligible, DSBs arise practically from single tracks only. For each value of R, the dependence of the DSB yields on R is almost linear. The linearity is most evident in Fig. 3 graphs, where the DSBs are represented as a function of the dose in the nucleus. The number of DSBs per cell per unit nucleus dose induced by tritium-derived beta particles is about 50 DSBs/Gy.

In addition to the information on the dose deposited and the total number of DSBs created from the radionuclide present within the cell, we performed a qualitative analysis on the type of damage induced by the radiation, in terms of DNA fragmentation patterns. Figure 4 represents the variation in the number of fragments (per cell) as a function of the average dose to the cell for different fragment intervals (0–30 bp, 30–1,000 bp, 1–9 kbp, 9–23.1 kbp, 23.1–1000 kbp, 1–5.7 Mbp and >5.7 Mbp), where the 0–30 bp interval corresponds to fragments from DSBs producing complex lesions (CLs), operationally defined as two or more DSBs within 30 bp (*35*).

In all the figure graphs there is a comparison of four different values of R: from which (0) corresponds to emitters only in the cytoplasm; up to R: (1) which describes uniformly distributed emitters. The expected dose dependence captured in these figure graphs is linear, since the contribution of multi-track effects to DSB induction and hence DNA fragmentation is negligible, as discussed above. The linearity is evident especially for larger fragments, where the fragment numbers are sufficiently high. However, it is notable that in all intervals the error bars are quite large, because relatively low doses and small cell numbers were used for the simulations, so that the fragment numbers obtained in each interval are not high enough to significantly reduce the stochastic variations. Also of note is that the number of CLs (i.e., fragments below 30 bp) per unit dose is about 0.1–0.5 CL/Gy, largely varying with the nucleus-to-cytoplasm ratio R (Fig. 4, top panel). The extraordinarily large value at 0.5 Gy (1 CL/Gy for $R = 1$) is likely an artifact of the discussed above small statistics only.

Figure 5 represents the simulation results for the cumulative distributions of DNA fragments induced by the electron tracks from the decay of tritium for different values of nucleus-to-cytoplasm ratio, at a nucleus dose of 16 Gy. As expected, the number of fragments in each interval increases with increasing numbers of tracks in the nucleus and thus with the R value. Taken together, Figs. 5 and 6 demonstrate the importance of considering the distribution of radionuclides within the cell, especially for nuclides emitting short-range electrons such as tritium.

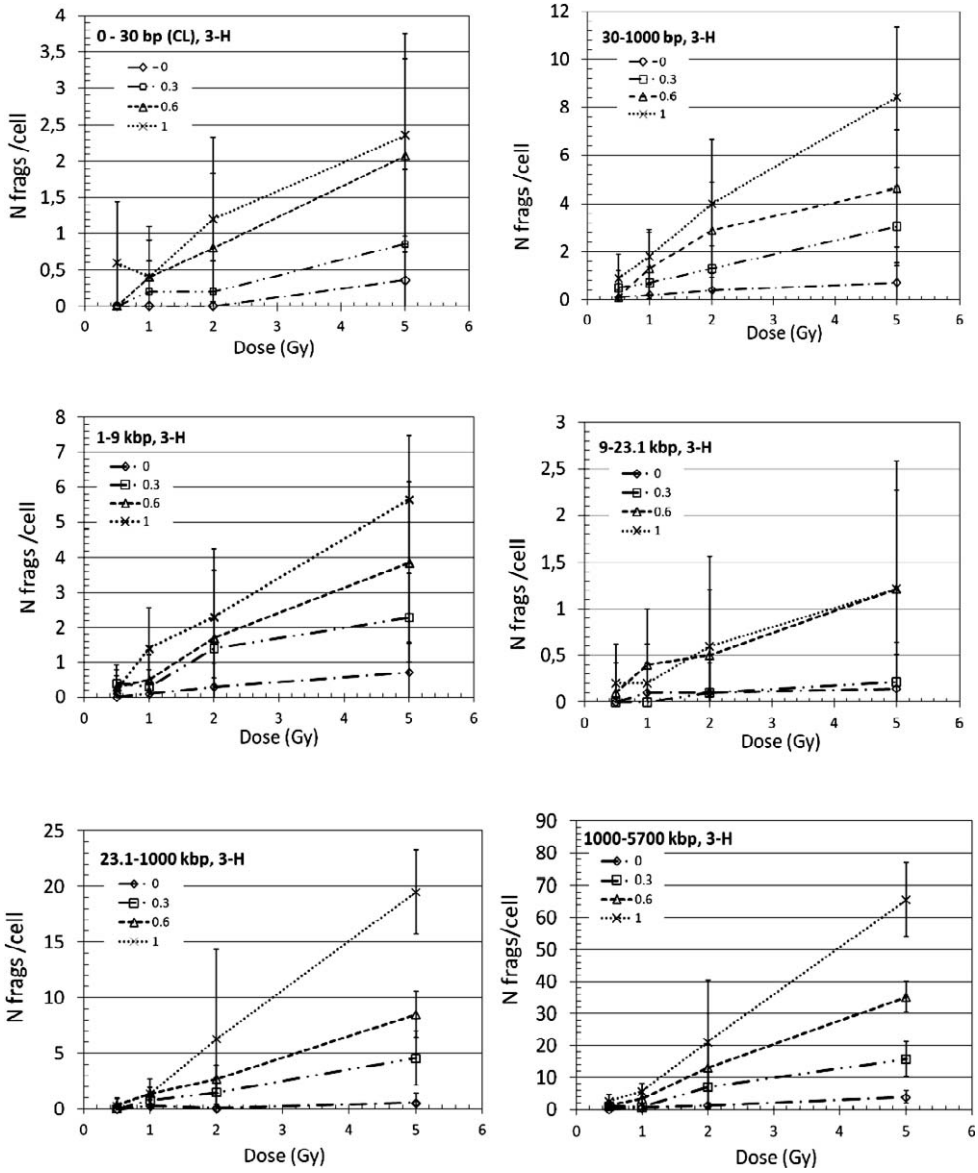

FIG. 4. Number of DNA fragments in different length ranges (as shown in the text) per cell as a function of the mean dose to the cell for tritium. Lines are drawn to guide the eye.

DISCUSSION

Simulations for Different 63Ni Concentrations in the Cell Nucleus

The simulated nucleus doses for ^{63}Ni for four different cell doses and varying nucleus-to-cytoplasm location ratio R of the emitter are shown in Fig. 2b. As was the case for tritium, the simulations for nickel-63 confirm the expected trend of linearity between the dose to the nucleus and the concentration ratio R. The intercept value for ^{63}Ni, which is 3.40 Gy for a cell dose of 5.33 Gy, i.e., 64% of the cell dose, corresponds to the energy imparted to the cell nucleus by electrons generated in the cytoplasm. This value is higher than that corresponding to tritium (0.82 Gy; Fig. 2e), because of the larger range of the electrons emitted from nickel. Therefore, even the tracks generated far from the nuclear membrane can reach the nucleus. The length of the tracks can reach values on the order of a few tens of μm (50/60 keV), but on average it is smaller, about 5 μm, considering that the average energy for the electrons is about 17 keV.

Induction of DSB and DNA Fragment Distributions

The relationship between the DSB numbers and the distribution of the beta emitters within the cell for different doses, shown in Fig. 2D, is approximately linear. Of note, the errors associated with each point in the graph, which were obtained by averaging the results of ten simulations, are larger than those obtained in Fig. 3 for tritium. This is due to the average energy of electrons emitted from nickel-63 being significantly larger than those from

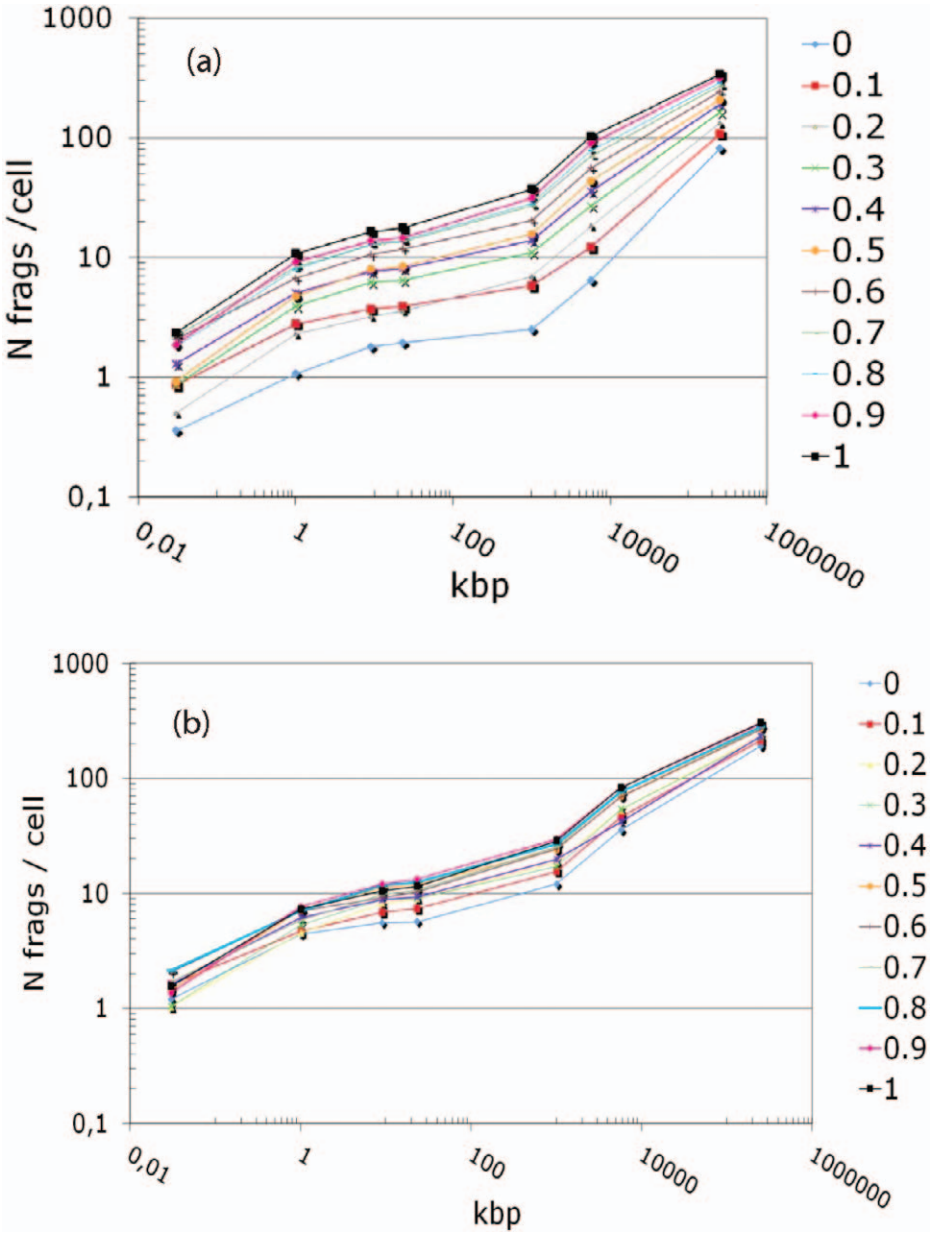

FIG. 5. Cumulative DNA fragment spectra for different values of *R* for tritium (panel a) and for nickel (panel b). Lines are drawn to guide the eye.

tritium, 17 keV vs. 5.7 keV, so that about threefold smaller numbers of tracks were simulated for nickel as compared to tritium.

Simulation results for the cumulative distribution of DNA fragments induced by the electrons from the decay of nickel-63 for different values of *R* are plotted in Fig. 5b. Again, the dependence on the distribution of emitters is less pronounced with respect to the case of tritium.

DSB Distribution in Chromosomes

The DSBs induced by the internal emission exposure have been analyzed with respect to the chromatin regions where they occur. Of particular interest is scoring the DSB numbers on individual chromosomes in different scenarios. Histograms that represent the simulation results for nickel-63 for two limiting emitter distributions, namely homogeneous in cytoplasm only (no incorporation into nucleus at all) or homogeneous in the whole cell, are shown in Fig. 6. For comparison, we also show the results of a theoretical calculation assuming a homogeneous spatial distribution of chromosomes in the cell nucleus and a homogeneous distribution of DSBs. Under these assumptions, the DSB numbers on individual chromosomes would be proportional to the chromosome size. The data with the label *random breakage* are thus obtained from the average number of DSBs obtained (842 DSBs per about 16 Gy cell dose being

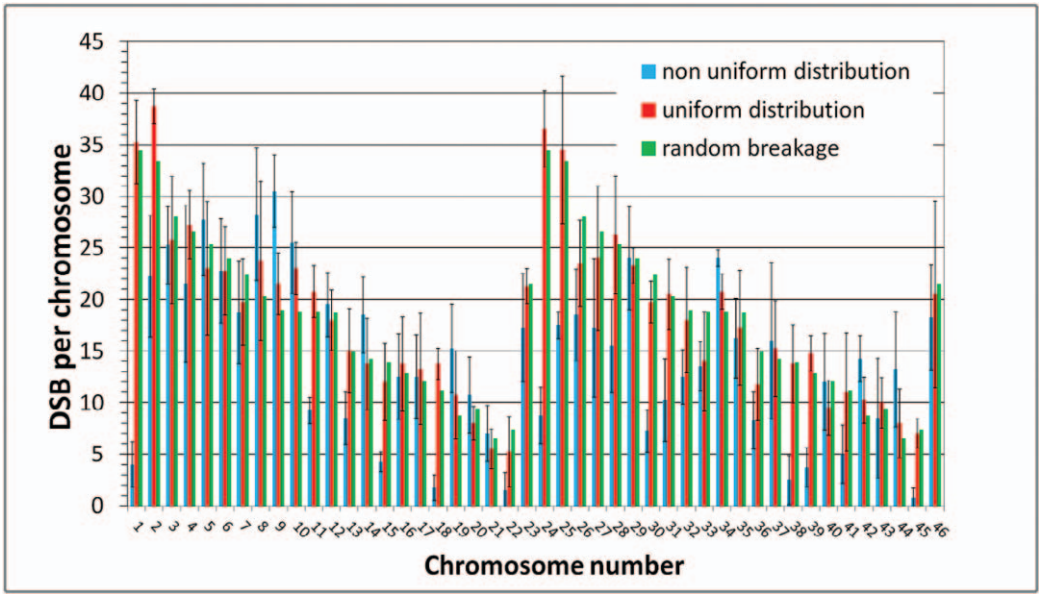

FIG. 6. Distribution of DSB number in each chromosome for uniform and nonuniform radiation conditions due to nickel-63 beta decay compared with random breakage data.

the average of ten simulations performed) multiplied by the length of each chromosome and divided by the genome length (6,425 Mbp). Apart from a few exceptions presumably of stochastic origin, the DSB numbers induced on individual chromosomes from the radionuclides confined to cytoplasm are generally smaller than those for the uniform emitter distribution. For the uniform distribution of the emitter, the simulated DSB distributions closely correspond to random breakage. For emitters confined to cytoplasm, however, the DSB distribution among chromosomes deviates significantly from random breakage. This reflects the actual intranuclear localization of the chromosomes. In the chromatin model underlying the reported simulations, some chromosomes (e.g., chromosome 1 or 11) are placed more centrally in the nucleus, whereas others (e.g., chromosome 21) more peripherally. Of note, the preference for a central or peripheral position is not an artifact of the chromatin model in PARTRAC, but a well-documented phenomenon in cell nuclei, is gene-dense chromosomes localize in the interior and gene-poor chromosomes towards the periphery of the nucleus (*32*). For emitters confined to the cytoplasm, due to the relatively short range of the beta particles from low-energy beta emitters, peripherally located chromosomes are hit by more electron tracks and hence exhibit more damage than central ones. As expected, the effects are even more pronounced for emitters with shorter electron ranges, such as tritium. Explicitly accounting for the nuclear-to-cytoplasm distribution of radionuclides is especially important if specific chromosome aberrations involving given chromosomes are to be predicted, e.g., aberrations involving chromosomes 4 and 18 (*36*).

CONCLUSIONS

The current work highlights the necessity to explicitly consider intracellular localization of low-energy beta emitters, such as ^{63}Ni or tritium, which emit electrons with average ranges of about 5 μm and 0.4 μm, respectively. For emitters that are distributed homogeneously in the whole cell, based on the biochemical properties of compounds of which they are a part, cellular doses as estimated from conventional protocols are a reasonable descriptor of energy deposition (dose) to the cell nucleus as well, and are therefore relevant for biological effects. For emitters that cannot pass through the nuclear membrane but remain confined to the cytoplasm, however, the nuclear dose may be as low as 15% of the cell dose. The nuclear dose, in turn, determines the biological effects, such as: DSB yields, DNA fragmentation or the yields of complex lesions, which correlate with later end points of chromosome aberrations or cell killing.

The current analysis can be further extended to other internal low-energy beta emitters, for example, for studies on radiation protection or metabolic radiotherapy. The same approach can also be used to estimate the effectiveness of boron carriers for BNCT (Boron Neutron Capture Therapy). The products of the neutron capture reaction ($n + {}^{10}B \rightarrow {}^{7}Li + \alpha$) have energy equal to 0.84 and 1.47 MeV, respectively, and release their energy within a few micrometers (4 and 6.5 μm), so that effects similar to those reported here for ^{63}Ni decay can be expected.

For future developments in nuclear medicine, the emitter as well as the biochemistry of organic compounds to which the radionuclides are bound will be of fundamental importance. The tendency for these compounds to concentrate in different regions of the cell may lead to damage of

different extents, especially for very low-energy internal emitters.

ACKNOWLEDGMENTS

This work was partially funded by EU (EC Contracts FP7 249689, DoReMi and 295970, ANDANTE). We would like to thank Drs. Pavel Kundrat and Giorgio Baiocco for their comments and suggestions.

Received: January 8, 2014; accepted: May 22, 2014; published online: August 12, 2014

REFERENCES

1. Zanzonico PB. Internal radionuclide radiation dosimetry: a review of basic concepts and recent developments. J Nucl Med 2000; 41:297–308.
2. Sgouros G. Toward patient-friendly cell-level dosimetry. J Nucl Med 2007; 48:496–7.
3. Sgouros G. Dosimetry of internal emitters. J Nucl Med 2005; 46, Suppl 1:S18–27. Review.
4. Paquet F, Houpert P, Verry M, Grillon G, Harrison JD, M'etivier H. The gastrointestinal absorption of ^{63}Ni and ^{95}Nb in adult and neonatal rats: effect of the chemical form administered. Radiat Prot Dosim 1998; 79:191–5.
5. Furhang EE, Chui CS, Kolbert KS, Larson SM, Sgouros G. Implementation of a Monte Carlo dosimetry method for patient-specific internal emitter therapy. Med Phys 1997; 24:1163–72.
6. Dandamudi VR, Roger WH, Venkateswara RN, George FG, Kandula SR. In-vivo radiotoxicity of DNA-incorporated 125I compared with that of densely ionising alpha-particles. Lancet 1989; 334:650–3.
7. Report of the Committee Examining Radiation Risks of Internal Emitters. London: CERRIE; 2004. (http://www.rachel.org/lib/cerrie_report.041015.pdf)
8. Hofer KG, Keough G, Smith JM. Biological toxicity of Auger emitters: molecular fragmentation vs. electron irradiation. Curr Top Radiat Res Q 1977; 12:335–68.
9. Charlton DE, Martin RF, Terrissol M, et al. Recent progress in the physics of Auger electrons. In: Hagan U, Harder D, Jung H, Streffer C, eds. Radiation research 1895–1995, 10th ed, vol. 2. Würzburg, 1995.
10. Taleei R, Nikjoo H. Repair of the double-strand breaks induced by low energy electrons: A modelling approach. Int J Radiat Biol 2012; 88:948–53.
11. Taleei R, Nikjoo H. The non-homologous end-joining (NHEJ) pathway for the repair of DNA double-strand breaks: I. A mathematical model. Radiat Res 2013; 179:530–9.
12. Taleei R, Girard PM, Sankaranarayanan K, Nikjoo H. The non-homologous end-joining (NHEJ) mathematical model for the repair of double-strand breaks: II. Application to damage induced by ultrasoft X rays and low-energy electrons. Radiat Res 2013; 179:540–8.
13. Liamsuwan T, Emfietzoglou D, Uehara S, Nikjoo H. Microdosimetry of low-energy electrons. Int J Radiat Biol 2012; 88:899–907.
14. Bousis C, Emfietzoglou D, Hadjidoukas P, Nikjoo H. Monte Carlo single-cell dosimetry of Auger-electron emitting radionuclides. Phys Med Biol 2010; 55:2555–72.
15. Alloni D, Campa A, Friedland F, Mariotti LG, Ottolenghi A. Track structure, radiation quality and initial radiobiological events: considerations based on the PARTRAC code experience. Int J Radiat Biol 2012; 88:77–86.
16. Alloni D, Campa A, Belli M, Esposito G, Mariotti L, Liotta M, et al. Monte Carlo evaluation of DNA fragmentation spectra induced by different radiation qualities. Radiat Prot Dos 2011; 143: 226–31.
17. Friedland W, Dingfelder M, Kundrát P, Jacob P. Track structures, DNA targets and radiation effects in the biophysical Monte Carlo simulation code PARTRAC. Mutat Res 2011; 711:28–40.
18. Day P. Radiation Dosimetry: why internal emitters are different, 2006. (http://www.bandepleteduranium.org/en/docs/97.pdf)
19. 19. Subgroup on Tritium Internal Dosimetry of the Advisory Group on Ionising Radiation. Review of risks from tritium. Oxfordshire: Health Protection Agency; 2007. (http://www.hpa.org.uk/webc/HPAwebFile/HPAweb_C/1197382221858).
20. Diabate S, Strack S. Organically bound tritium. Health Phys 1993; 65:698–712.
21. Hamoudeh M, Kamleh MA, Diab R, Fessi H. Radionuclides delivery systems for nuclear imaging and radiotherapy of cancer. Adv Drug Deliver Rev 2008; 60:1329–46.
22. 22. European Commission Radiation Protection. Emerging issues on tritium and low energy beta emitters. Report No. 152. Proceedings of the EU Scientific Seminar; 2007; Luxembourg. (http://ec.europa.eu/energy/nuclear/radiation_protection/doc/publication/152.pdf)
23. U.S. Department of Energy. DOE handbook: Primer on tritium handling and safe storage. Washington, D.C.: U.S. Department of Energy; 2008. (http://energy.gov/sites/prod/files/2013/07/f2/hdbk1129.pdf)
24. Saito M, Ishida MR. Dose-modification factor for accumulated dose to cell nucleus due to protein-bound 3H. Health Phys 1989; 56:869–74.
25. Taylor DM, Moroni JP, Snihn JO, Richmond CR. The metabolism of 3H and 14C with special reference to radiation protection. Radiat Prot Dosim 1990; 30:87–93.
26. Limits for intakes of radionuclides by workers. ICRP Publication 30. New York: Pergamon Press; 1979–1982.
27. Carboneau ML, Adams JP. National low-level waste management program radionuclide report series; Volume 10: Nickel-63. Washington, D.C.: U.S. Department of Energy; 1995.
28. Cross WG, Ing H, Freedman N. A short atlas of beta-ray spectra. Phys Med Biol 1983; 28:1251–60.
29. 29. International Atomic Energy Agency. Safe handling of radioisotopes. Vienna, Austria: IAEA; 1958.
30. Richardson RB, Dubeau J, Trivedi A. Dose to the cell nucleus from exposure to tritiated pump oil or formaldehyde. Health Phys 2000; 78:672–8.
31. Ballarini F, Biaggi M, Merzagora M, Ottolenghi A, Dingfelder M, Friedland W, et al. Stochastic aspects and uncertainties in the prechemical and chemical stages of electron tracks in liquid water: a quantitative analysis based on Monte Carlo simulations. Radiat Environ Biophys 2000; 39:179–88.
32. Cremer M, von Hase J, Volm T, Brero A, Kreth G, Walter J, et al. Non-random radial higher-order chromatin arrangements in nuclei of diploid human cells. Chrom Res 2001; 9:541–67.
33. Kreth G, Pazhanisamy SK, Hausmann M, Cremer C. Cell type-specific quantitative predictions of radiation-induced chromosome aberrations: a computer model approach. Radiat Res 2007; 167:515–25.
34. Friedland W, Paretzke HG, Ballarini F, Ottolenghi A, Kreth G, Cremer C. First steps towards systems radiation biology studies concerned with DNA and chromosome structure within living cells. Radiat Environ Biophys 2008; 47:49–61.
35. Ballarini F, Merzagora M, Monforti F, Durante M, Gialanella G, Grossi GF, et al. Chromosome aberrations induced by light ions: Monte Carlo simulations based on a mechanistic model. Int J Radiat Biol 1999; 75:35–46.
36. Kreth G, Pazhanisamy SK, Hausmann M, Cremer C. Cell type-specific quantitative predictions of radiation-induced chromosome aberrations: a computer model approach. Radiat Res 2007; 167:515–25.